MID-AMERICA TRANSPORTATION CENTER

Report # MATC-MS&T: 136-2

Final Report
WBS: 25-1121-0005-136-2

Performance Investigation of Earthquake Damaged Reinforced Concrete Bridges with Repaired Columns

Lesley H. Sneed, PhD
Professor
Department of Civil, Materials, and Environmental Engineering
University of Illinois at Chicago
Adjunct Professor
Department of Civil, Architechural, and Environmental Engineering
Missouri University of Science and Technology

Giacomo Fraioli
Graduate Research Assistant
Department of Civil, Architectural, and Environmental Engineering
Missouri University of Science and Technology

2021

A Cooperative Research Project sponsored by
U.S. Department of Transportation- Office of the Assistant Secretary for Research and Technology

Performance Investigation of Earthquake-Damaged Reinforced Concrete Bridges with Repaired Columns

Giacomo Fraioli
Graduate Research Assistant
Department of Civil, Architectural and Environmental Engineering
Missouri University of Science and Technology, Rolla, MO

Lesley H. Sneed, Ph.D., P.E., S.E.
Professor
Department of Civil, Materials and Environmental Engineering
University of Illinois at Chicago, Chicago, IL
Adjunct Professor
Department of Civil, Architectural and Environmental Engineering
Missouri University of Science and Technology, Rolla, MO

A Report on Research Sponsored by

Mid-America Transportation Center

University of Nebraska–Lincoln

June 2021

Technical Report Documentation Page

1. Report No. 25-1121-0005-136-2	2. Government Accession No.	3. Recipient's Catalog No.
4. Title and Subtitle Performance Investigation of Earthquake-Damaged Reinforced Concrete Bridges with Repaired Columns		5. Report Date June 2021
		6. Performing Organization Code
7. Author(s) Giacomo Fraioli, Lesley H. Sneed, Ph.D, http://orcid.org/0000-0003-1528-5611		8. Performing Organization Report No. 25-1121-0005-136-2
9. Performing Organization Name and Address Missouri University of Science and Technology, Rolla, MO		10. Work Unit No. (TRAIS)
		11. Contract or Grant No. 69A3551747107
12. Sponsoring Agency Name and Address Mid-America Transportation Center 2200 Vine St. PO Box 830851 Lincoln, NE 68583-0851		13. Type of Report and Period Covered Final report (Jan 2019-June 2021)
		14. Sponsoring Agency Code MATC TRB RiP No. 91994-43
15. Supplementary Notes Conducted in cooperation with the U.S. Department of Transportation, Federal Highway Administration.		

16. Abstract

This report summarizes the details of a study that was conducted to determine the influence of a column repair (member level) on the post-repair performance of bridge structures (system level). Reinforced concrete (RC) bridge columns are typically designed to be the primary source of energy dissipation for a bridge structure during an earthquake. Therefore, seismic repair of RC bridge columns has been studied extensively during the past several decades; however, few studies have been conducted evaluate how repaired column members effect the system-level response of an RC bridge structure in subsequent earthquakes. In this study, a numerical model was established to simulate the response of two repaired RC columns reported in the literature. The columns were implemented into a prototype bridge that was subjected to earthquake loading. Incremental dynamic analysis (IDA) was conducted on numerical bridge models to evaluate the efficacy of the repair and the post-repair seismic performance of the prototype bridge that included one or more repaired columns. The methodology adopted in this study was based on previous work by He et al. (2016) and was extended to RC columns with different repair conditions.

17. Key Words Columns, Reinforced Concrete Bridges, Earthquake damage, Incremental Dynamic Analysis, Repairing	18. Distribution Statement No restrictions.		
19. Security Classif. (of this report) Unclassified	20. Security Classif. (of this page) Unclassified	21. No. of Pages 52	22. Price

Table of Contents

List of Figures

List of Tables

List of Abbreviations

Carbon fiber reinforced polymer (CFRP)
Cast in place (CIP)
Damage measure (DM)
Damage state (DS)
Externally bonded (EB)
Fiber reinforced polymer (FRP)
Glass fiber reinforced polymer (GFRP)
Ground motion (GM)
Incremental dynamic analysis (IDA)
Intensity measure (IM)
Mid-America Transportation Center (MATC)
Missouri University of Science & Technology (Missouri S&T)
Open System for Earthquake Engineering Simulation (OpenSees)
Pacific Earthquake Engineering Research (PEER)
Reinforced concrete (RC)

Acknowledgments

Funding provided for this research was sponsored by the Mid-America Transportation Center (MATC). The project was entirely developed in the Civil, Architectural and Environmental Engineering Department of the Missouri University of Science & Technology (Missouri S&T). The authors would also like to acknowledge Dr. Yang Yang (University of Hartford) for his input regarding the numerical simulation.

Disclaimer

The contents of this report reflect the views of the authors, who are responsible for the facts and the accuracy of the information presented herein. This document is disseminated in the interest of information exchange. The report is funded, partially or entirely, by a grant from the U.S. Department of Transportation's University Transportation Centers Program. However, the U.S. Government assumes no liability for the contents or use thereof.

Abstract

This report summarizes the details of a study conducted to determine the influence of a column repair (member level) on the post-repair performance of bridge structures (system level). Reinforced concrete (RC) bridge columns are typically designed to be the primary source of energy dissipation for a bridge structure during an earthquake. Therefore, seismic repair of RC bridge columns has been studied extensively during the past several decades; however, few studies have been conducted to evaluate how repaired column members effect the system-level response of an RC bridge structure in subsequent earthquakes. In this study, a numerical model was established to simulate the response of two repaired RC columns reported in the literature. The columns were implemented into a prototype bridge that was subjected to earthquake loading. Incremental dynamic analysis (IDA) was conducted on numerical bridge models to evaluate the efficacy of the repair and the post-repair seismic performance of the prototype bridge that included one or more repaired columns. The methodology adopted in this study was based on previous work by He et al. (2016) and was extended to RC columns with different repair conditions.

Chapter 1 Introduction

In vehicular bridge structures, column members are typically designed to be the primary source of energy dissipation during an earthquake. Therefore, reinforced concrete (RC) bridges that are damaged in an earthquake tend to have damage to the column members. According to the current seismic design practice, RC bridge columns can undergo cracking, spalling, or crushing of concrete, or yielding of reinforcing bars depending on the performance level of a bridge specified by the bridge owner or administrative agency. In the most extreme scenarios, bar buckling, or fracture may also occur when the earthquake effects exceed the ultimate limit state.

Techniques to repair earthquake-damaged RC bridge columns include injection of concrete cracks (French et al. 1990), replacement of damaged concrete, and/or application of external jackets. Moreover, RC (Lehman et al. 2001), steel (Fukuyama et al. 2000), and fiber reinforced polymer (FRP) (Vosooghi and Saiidi 2009) are commonly used as jacketing materials to provide external reinforcement and/or confinement of the concrete. The repair system selected depends on many factors including time/ease of installation (important for rapid repair), cost, long-term durability (important for a permanent repair), and level of performance that can be achieved by the repaired member (important for both rapid and permanent repairs) (Sneed et al. 2019). However, the use of a repair method can change the performance of the RC column. For example, it has been shown that certain repair methods cannot restore the initial stiffness of damaged RC columns to the undamaged-unrepaired state (He et al. 2013, Fakharifar et al. 2015), and some repair methods do not restore the same level of energy dissipation capability. Changes in column performance in terms of strength, stiffness, and ductility are a function of the type of

repair method used as well as the extent of repair along the member length. These changes can, in turn, influence the bridge structure performance, especially under seismic loading.

Most previous research on seismic repair of RC bridges was focused on evaluating the response of individual columns (member level), not the bridge structure (system level), due to limitations in modeling and especially testing of full bridge structures. Thus, the need exists to develop techniques to understand the effects of the repair on the performance of the entire bridge structure. Moreover, since each repair is unique and involves complex combinations of original and repair materials, member geometry and reinforcement, initial damage, and repair procedure, it is impractical to study the topic purely on an experimental basis. The availability of increasingly powerful computers provides an opportunity to implement numerically intensive modeling strategies. Analytical tools, such as those based on the fiber element method, have been developed to model the nonlinear behavior of RC structures subjected to cyclic loading. Moreover, studies have shown the fiber element method can be effective in simulating the response of RC members and bridge structures under seismic loading (Shao et al. 2005, Zhu et al. 2006, He et al. 2016).

The objective of this project was to develop a framework to investigate how local modifications to individual RC bridge columns effect the post-repair seismic performance of a bridge structure. Knowledge of the post-repair seismic performance of a bridge system is needed to effectively design either a permanent repair to restore/improve the bridge seismic performance or a rapid repair to enable limited access or mitigate further damage due to aftershocks.

The influence of the member level repair on the performance of the bridge system was investigated using experimental studies conducted on RC bridge columns. Two large-scale RC bridge column tests with different damage conditions and repair methods were selected from the

literature. Currently available techniques were used to model the undamaged and repaired columns (He et al. 2016). The models were developed using Open System for Earthquake Engineering Simulation (OpenSees) (McKenna et al. 2000) and were validated by comparing the calculated responses with the measured test data. Then, a prototype bridge with four columns was selected from the literature, and its dynamic response was numerically simulated and validated. Finally, incremental dynamic analysis (IDA) was conducted to evaluate the post-repair seismic performance of an RC bridge structure that included one or more repaired columns. The methodology adopted in this study was previously established by (He et al. 2016) and was extended in this work to investigate the performance of different RC column repair systems.

Chapter 2 Modeling of RC Bridge Columns

2.1 Overview

This section presents the numerical models of the undamaged (original) and repaired columns considered in this study. Two large-scale RC bridge column tests were selected from the literature to be modeled using the Open System for Earthquake Engineering Simulation (OpenSees) software framework (McKenna et al. 2000). Specimens selected for modeling were flexure-dominated and had the full hysteretic response of both the original and repaired columns reported so that the numerical model of the columns could be validated. In addition, all dimensions and material properties were reported. The two specimens chosen for the simulation had different damage conditions and repair strategies. The RC columns were modeled with the intent to evaluate the performance of the different repair strategies. The material models used in the simulation were selected from those available in OpenSees. The level of damage was considered by reducing the material properties as described in Vosooghi (2010). The models developed in this study followed the approach established by He et al. (2016), which proved to be capable of reproducing the response of a repaired column in terms of initial stiffness, base shear capacity, strength degradation, and stiffness degradation. The developed column models were then implemented in a model of a prototype bridge structure to investigate the post-repair seismic response of the bridge structure.

2.2 Modeling of the original and repaired columns

The columns were modeled as a fiber section object, in which the cross section is discretized into fibers, since studies have shown that the fiber element method can be effective in simulating the response of RC members under seismic loading (Shao et al. 2005, Zhu et al. 2006, Xiao and Ma 2005). Each fiber is characterized by a prescribed uniaxial material, an area, and a

location. The core concrete, cover concrete, and longitudinal steel fibers were defined by a uniaxial stress-strain model corresponding to the material they represent.

Confined and unconfined concrete was modeled in OpenSees using Linear Tension Softening Concrete02 material. The compressive stress–strain relationship of the material model is based on the uniaxial Kent–Scoff–Park concrete material model (Kent and Park 1971). The tensile stress–strain relationship is bilinear with the same modulus as the compressive elastic modulus. The effect of the confinement caused by the internal transverse reinforcement and by the FRP jacket was evaluated using Mander's model (Mander et al. 1988). Figure 2.1 shows the stress-strain relationship, as well as the input required, of the Concrete02 Material implemented in OpenSees.

The longitudinal reinforcing steel was modeled in OpenSees as Hysteretic material. This model was preferred to the uniaxial models available in OpenSees based on previous investigation on the capability to simulate the strength degradation due to bar fracture or buckling and to achieve convergence at large strains (He et al. 2016). The hysteretic material model requires three stress–strain inputs in both tension and compression to represent the monotonic behavior of the reinforcing steel. The cyclic behavior of the steel model is controlled by additional parameters px (pinching factor for strain during reloading), py (pinching factor for stress during reloading), D1 (damage due to ductility), D2 (damage due to energy), and β (power used to determine the degraded unloading stiffness based on ductility). The behavior of reinforcing steel in tension and compression was modeled with the same values. Figure 2.1 shows the stress-strain relationship, as well as the input needed, of the Hysteretic material implemented in OpenSees.

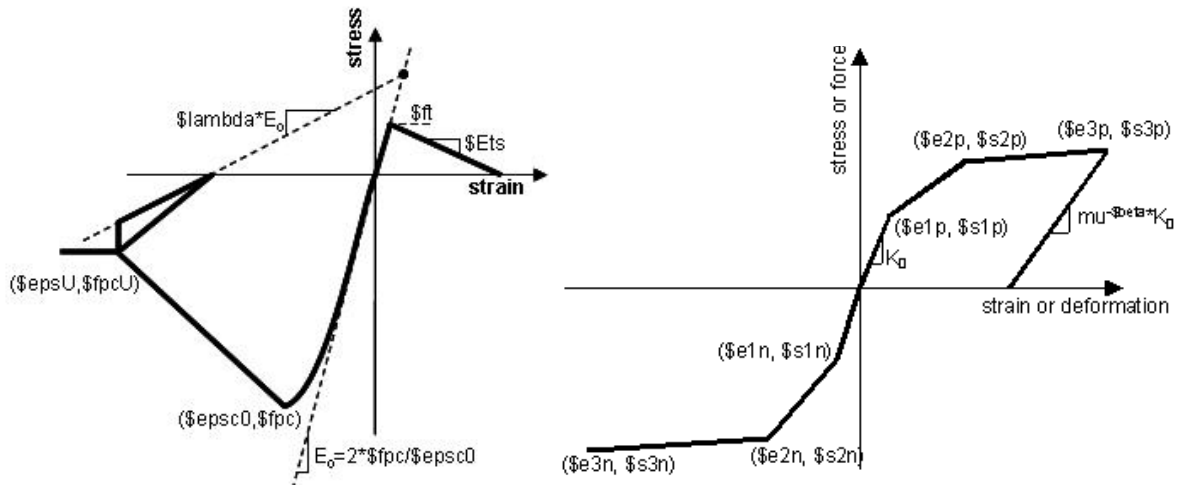

Figure 2.1 Concrete02 Material – Linear Tension Softening (left) and Hysteretic Material (right) (Mazzoni et al. 2006)

A study performed by Vosooghi and Saiidi (2010), based on the review of shake test data on 30 RC bridge columns, allowed the identification of five damage states (DS) corresponding to five apparent levels of damage: DS-1: flexural cracks; DS-2 first spalling and shear cracks; DS-3: extensive cracks and spalling; DS-4: visible transverse and longitudinal bars; and DS-5: imminent failure. Under DS-5, the most extreme damage state considered, only a few longitudinal bars may exhibit slight buckling with no appreciable impact on the ability of the column to carry axial load. In the case of the repaired columns, the reinforcing steel properties were modified according to the damage state as defined above to account for the effect of previous earthquake damage on the column (Vosooghi 2010). The Hysteretic material used to model the existing longitudinal bars in the repaired column was adjusted to modify the elastic modulus by applying reduction factors selected based on the damage state. This study implemented the factors suggest by Vosooghi (2010) with values of 0.67, 0.5, and 0.2 for damage states DS-2, DS-3, and DS-5, respectively.

For an RC column subjected to a lateral load, it is well established that the total lateral deflection can be attributed to deformations due to flexure, shear, and bond slip (Scott et. al 1982, Paulay and Priestley 1992). In this model, the shear and bond slip deformations were simulated by using zero-length springs, referred to as shear and bond–slip springs, respectively.

The shear spring was modeled as a ZeroLength element, in which the force–deformation relationship in the loading direction was modeled with the Hysteretic material. The force–deformation relationships in the other directions were modeled with elastic materials with a large elastic stiffness close to infinity to exclude the flexibility in those directions. In the Hysteretic model, a tri-linear curve was used to represent the backbone of the force–deformation relationship, for which values were obtained using the software Response 2000 (Bentz and Collins 2000).

The pinching effect and strength degradation were neglected in the cyclic behavior of the shear spring, and the unloading stiffness was kept as the initial elastic stiffness. The unloading stiffness in the shear spring cyclic behavior was kept as the initial elastic stiffness, while pinching effect and strength degradation were neglected.

To consider the bond slip from strain penetration effects, a bond-slip spring was added to the model. The bond–slip spring was modeled as a ZeroLengthSection element, where the section discretization of the element was the same as that of the column element. A stress-slip relationship was used to characterize the reinforcing steel. According to Zhao and Sritharan (2007), the relationship of bar stress versus loaded-end slip can be assumed as a linear relationship for the elastic region and a curvilinear relationship for the post-yield region.

2.3 Experimental Test A

2.3.1 Experimental description and column response

The first test selected for the simulation was carried out by Sheikh and Yau 2002. The test specimen, named R-1NT, was 1470 mm high and had a circular cross-section of 356 mm. Figure 2.2 shows the dimensions of the column and the layout of the internal reinforcement.

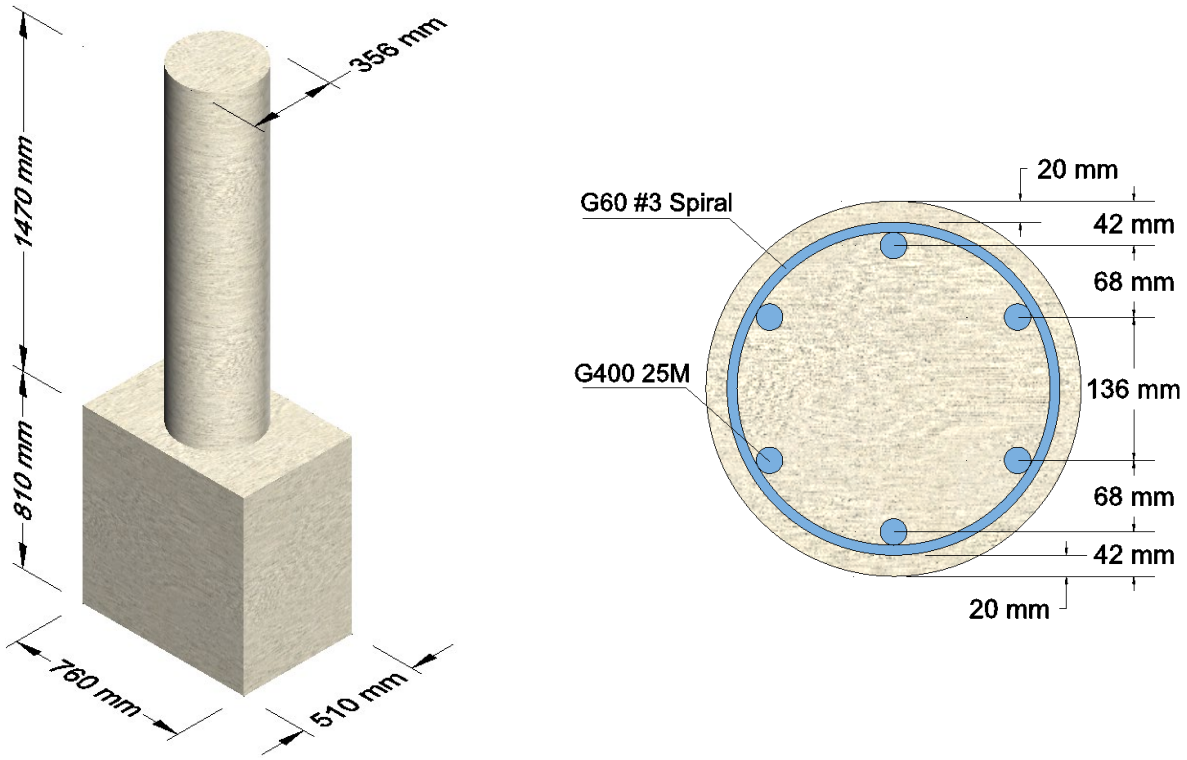

Figure 2.2 Experimental Test A: column and cross-section dimensions of specimens tested by Sheikh and Yau (2002)

The specimen was damaged to a certain extent under axial and lateral load, repaired under axial loads with a GFRP jacket, and then tested to failure. Both the original and repaired columns where subjected to inelastic cyclic loading while simultaneously carrying axial load

equal to $P = 0.54P_0$, where $P_0 = [0.85f'_c(A_g - A_s) + A_s f_y]$. The column was initially subjected to three load cycles with the lateral deflection Δ_1 calculated using the theoretical sectional behavior of the column and integrating curvatures along the length of the specimen (Sheikh and Yau 2002). Δ_1 was defined as the lateral deflection corresponding to the maximum lateral load along a line that represented the initial stiffness of the specimen (Sheikh and Yau 2002). The specimen was further damaged with two cycles of $1.4\Delta_1$. Flexural cracks were observed in the hinging zone at approximately 100 to 400 mm from the stub face. Some spalling of the top cover occurred at 435 to 685 mm from the stub. Yielding of longitudinal reinforcement was also observed.

After the original test was completed, the damaged column was repaired with a high-early strength mortar and confined with 2 layers of 1.25 mm thick GFRP while it was subjected to 2/3 of the original applied axial load. The repair mortar was cured two days before the GFRP was wrapped around the column. The loading protocol used to carry out the inelastic cyclic loading on the repaired column, shown in figure 2.3, consisted of one cycle to a displacement of $0.75\Delta_1$ (defined above) followed by two cycles each to $1\Delta_1$, $2\Delta_1$, $3\Delta_1$... and so on, until the specimen was unable to maintain the applied axial load.

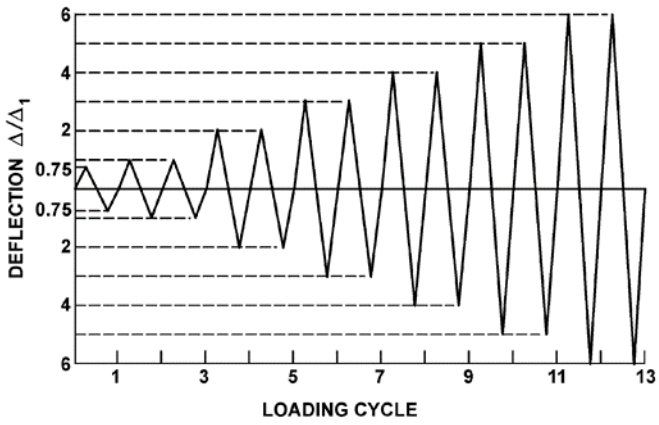

Figure 2.3 Experimental Test A: specified displacement history (Sheikh and Yau 2002)

During the test, the lateral load and section capacity of the repaired column increased with each load cycle until failure, which was caused by jacket opening. Figure 2.4 shows a photo of the repaired column at the end of the test. Figure 2.5 shows the cyclic behavior of both the original and repaired columns.

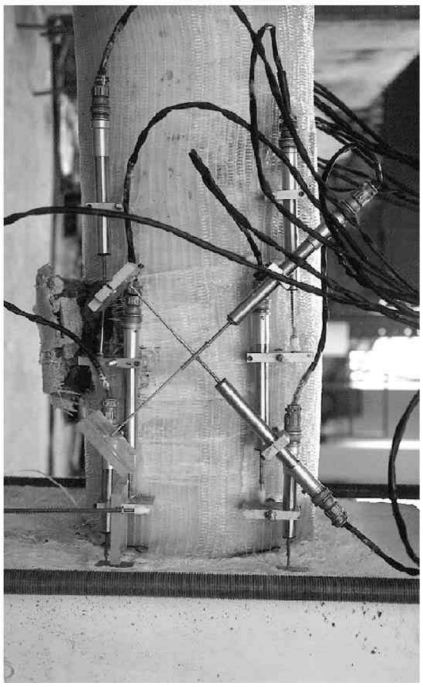

Figure 2.4 R-1NT repaired column failure (Sheikh and Yau 2002**)**

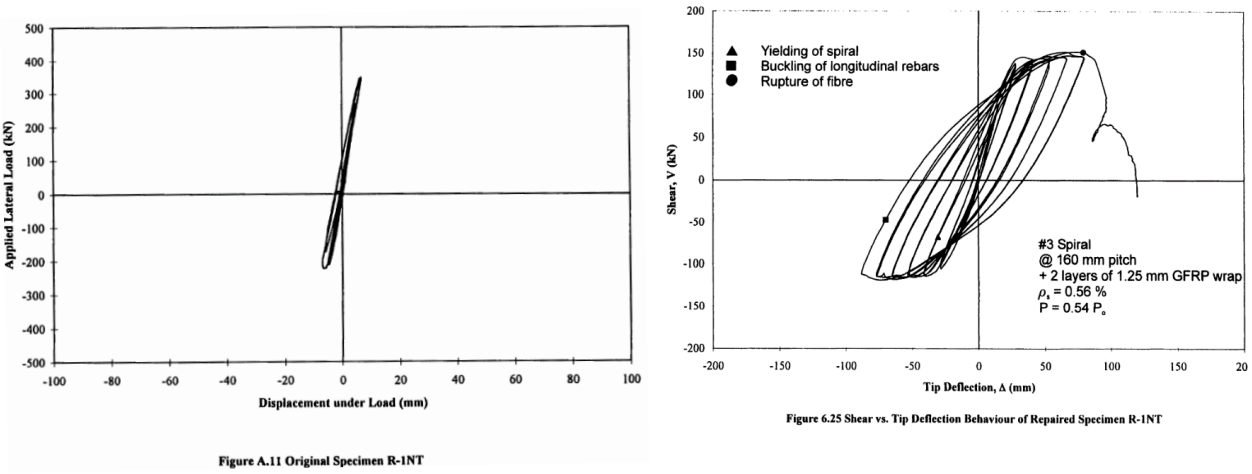

Figure 2.5 Experimental Test A: cyclic behavior of the original (left) and repaired (right) specimen (Yau 1998)

2.3.2 Column numerical model and validation

Both the original and repaired columns were modeled as a non-linear beam-column element with a fiber cross-section consisting of 12 subdivisions (fibers) in the circumferential direction and 24 subdivisions (fibers) in the radial direction. Figure 2.6 shows the column model and cross-section discretization. The repaired column, represented in figure 2.7, was wrapped by a GFRP jacket. Therefore, the cross-section was subdivided into two macro areas: the cover confined by the GFRP jacket, and the core confined by both the transverse reinforcement and the GFRP jacket.

Tested values of the material properties, reported in figure 2.8, were used to model the stress-strain curve of the reinforcing steel bars and effect of GFRP confinement. The compressive strength of concrete f'_c was reported as 42.8 MPa, while the GFRP tensile strength and modulus were 400 MPa and 20 GPa respectively.

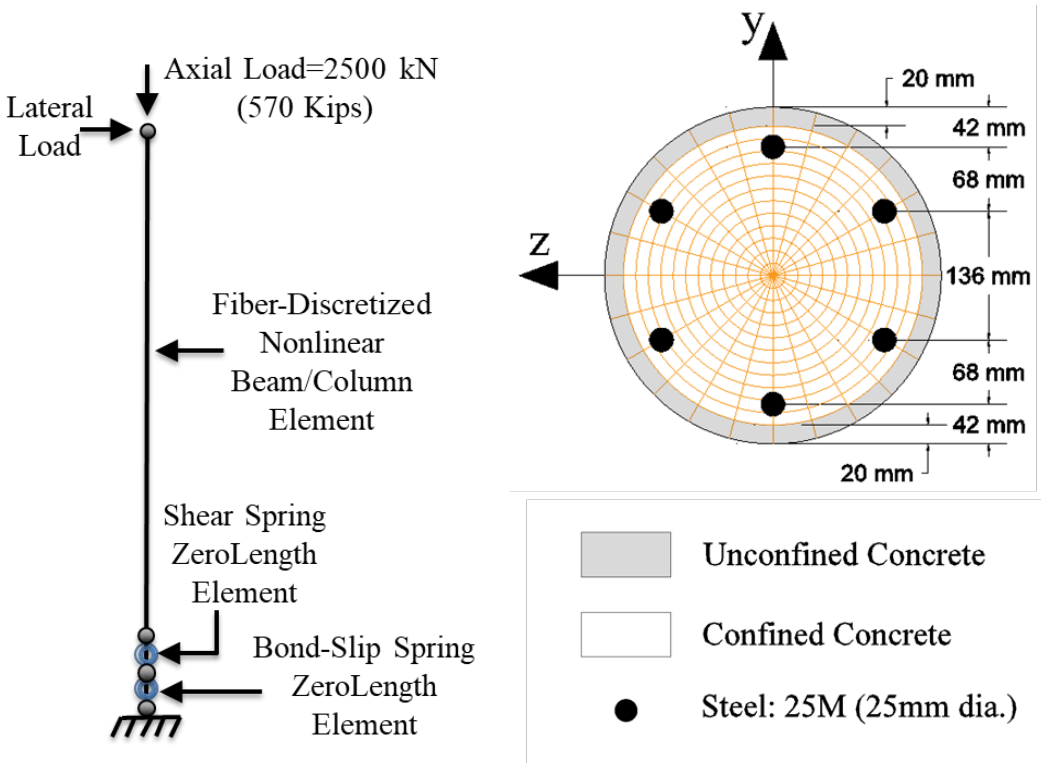

Figure 2.6 Test A: original column and cross section model

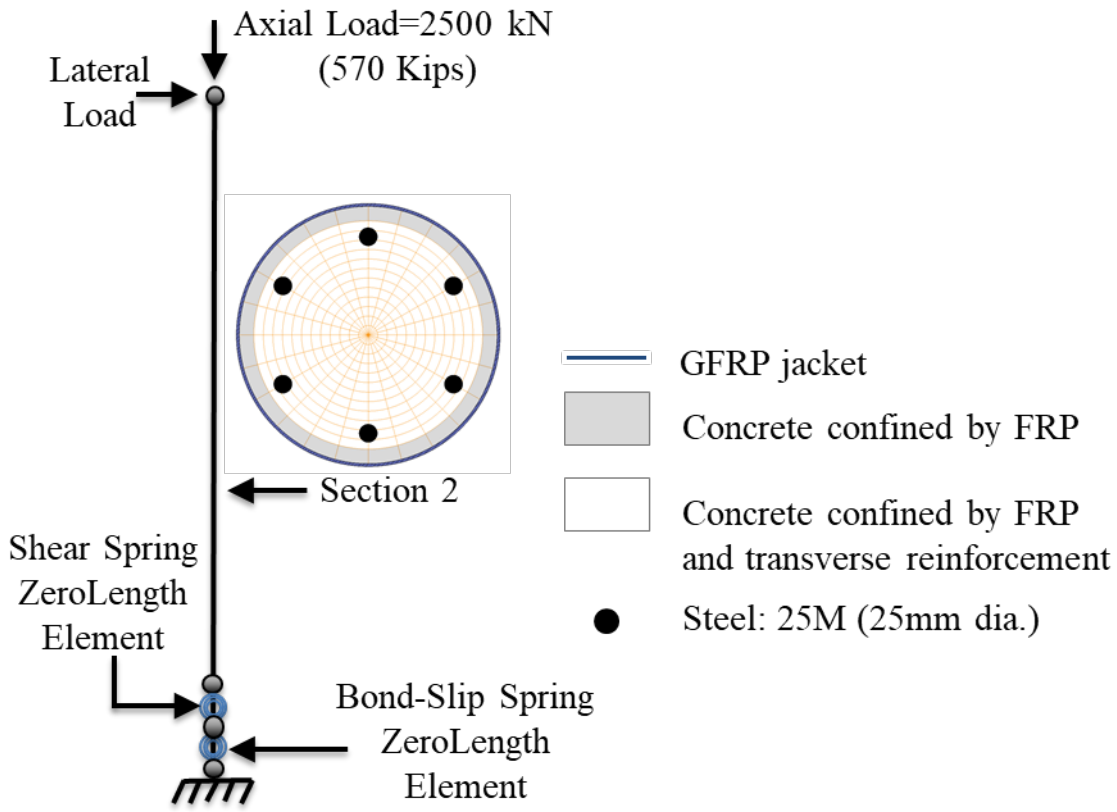

Figure 2.7 Experimental Test A: repaired column and cross section model

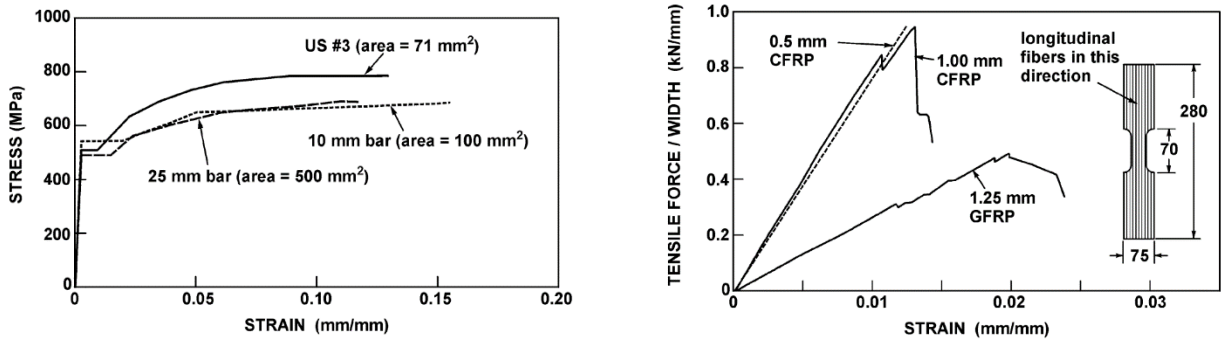

Figure 2.8 Experimental Test A: tensile stress-strain curves for reinforcing steel bars (left) and tensile force-strain curves for GFRP composite (Sheikh and Yau 2002)

The experimental cyclic test carried out on Test A was modeled in OpenSees according to the description in Section 2.2. The software was run on a workstation with an Intel Xenon processor with a speed of 3.6 GHz on a 64-b operating system. The program took approximately 1 minute. The analysis graphs presented below were obtained by plotting OpenSees output text files using MATLAB. In figures 2.8 and 2.9 the numerical results of Test A are shown and compared with the experimental backbone curves. The numerical results are in good agreement with the experimental results. These results show the repaired column can be simulated using the proposed approach.

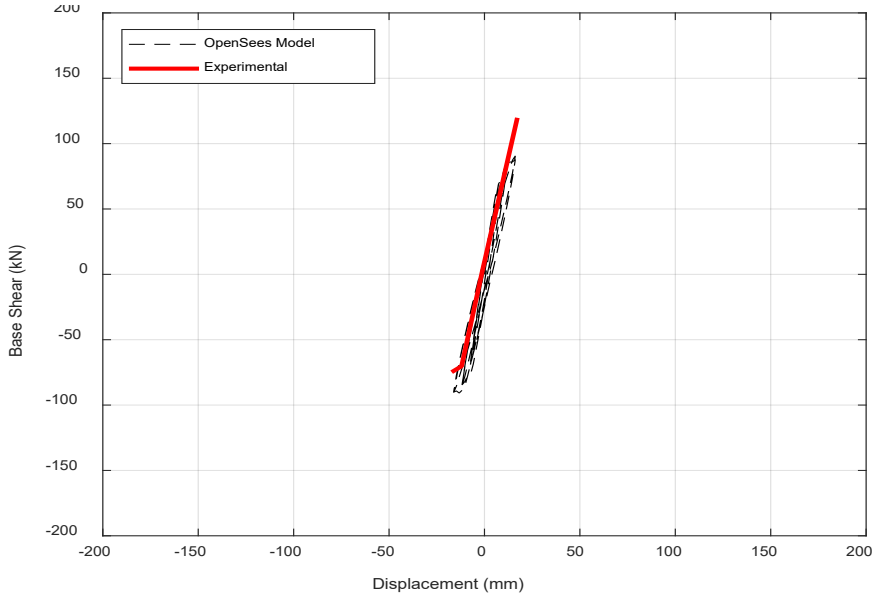

Figure 2.9 Test A: numerical and experimental cyclic behavior of original column

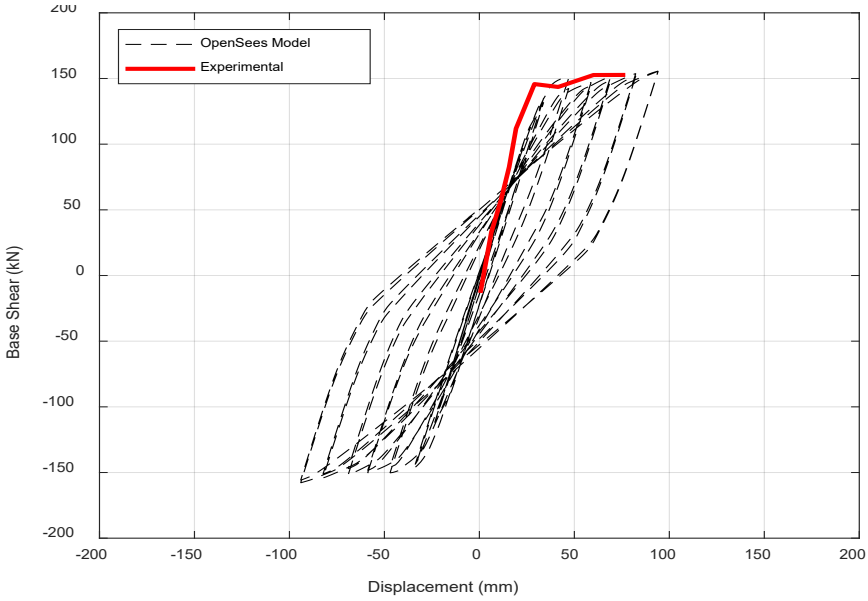

Figure 2.10 Test A: numerical and experimental cyclic behavior of repaired column

2.4 Experimental Test B

2.4.1 Experimental description and column response

The second test selected for the simulation was carried out by Rutledge et al. (2014), who investigated the behavior of single curvature bridge columns. The column, identified by Rutledge et al. (2014) as Specimen 2, was 2440 mm high and 600 mm in diameter. The cross-section longitudinal reinforcement consisted of 16 #6 (12.7 mm dia.) reinforcing steel bars, while the transverse reinforcement was a #3 (9.5 mm dia.) spiral with 50 mm pitch. Figure 2.10 shows the column dimensions and the location of reinforcement in the cross-section.

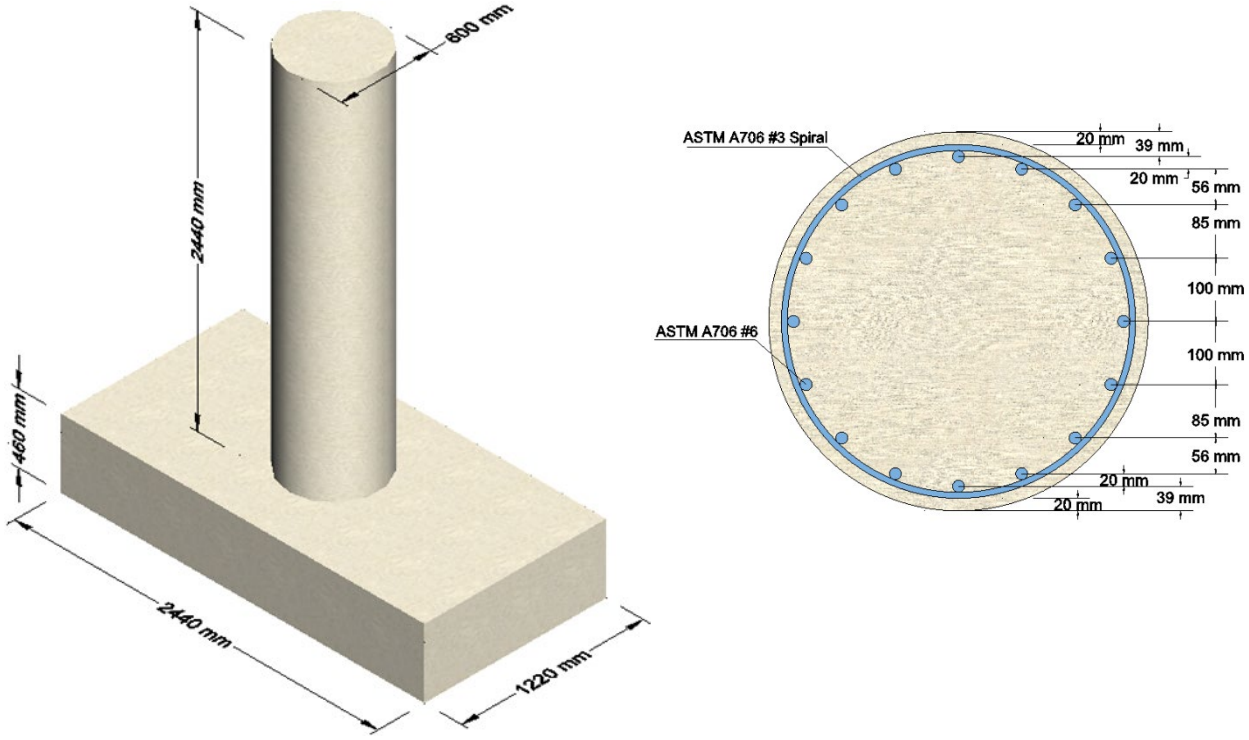

Figure 2.11 Experimental Test B: column and cross-section dimensions of the specimens tested by Rutledge et al. (2014)

Prior to repair, and in a different research program (Goodnight et al. 2012), the column was tested in a static manner using the top column displacement, obtained by nonlinear time history analysis of the column itself under the influence of the Chile 2010 earthquake, as a the actuator motion. Also prior to repair, the column was additionally subjected to a cyclic loading referred to as “cyclic aftershock” in accordance with the displacement history reported figure 2.11. At the end of the test, two buckled bars were noticed, while none fractured.

The damaged RC column was repaired by plastic hinge relocation using CFRP in the hoop and vertical directions, with the vertical CFRP anchored into the footing. Additional confinement was applied in the new hinge region using CFRP in the hoop direction. The design of the repair aimed to increase the flexural strength of the original hinge creating a capacity-

protected region. The repair procedure began by removing the loose concrete from the column and replacing it using a commercial cementitious system. The buckled longitudinal bars were not straightened out. The CFRP was applied using a wet layup technique. A single layer of vertical fibers was impregnated by epoxy resin and then applied onto the column from the base up to 600 mm around the circumference. The carbon fiber anchors were insert in evenly distributed holes drilled into the footing and with fans splayed on the column. Two more layers of vertical CFRP were subsequently applied on the region. The final step was to wrap the column up to 600 mm with six CFRP layers in the hoop direction.

The repaired column was subjected to a loading referred to as "Test two". During "Test two", the repaired column was subjected to displacement-controlled symmetric three-cycle load history while simultaneously carrying an axial load ratio ($P/f'_c'A_g$) of 6%, corresponding to 756 kN. The lateral load sequence, shown in figure 2.11, consisted of one cycle to a displacement $0.25F_y$, $0.50F_y$, $0.75F_y$, followed by three cycles of 1μ, 1.5μ, 2μ, 2.5μ, 3μ, 4μ, 6μ, 8μ,10μ, 12μ, where μ indicates the displacement ductility.

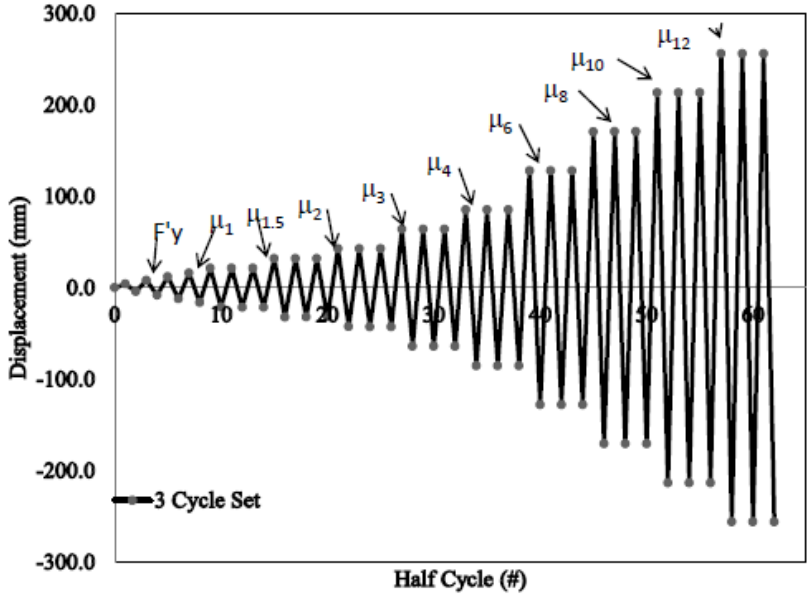

Figure 2.12 Experimental Test B: specified displacement history used during "Test two" (Rutledge 2012)

Figure 2.13 Experimental Test B: photo at peak displacement (Rutledge 2012)

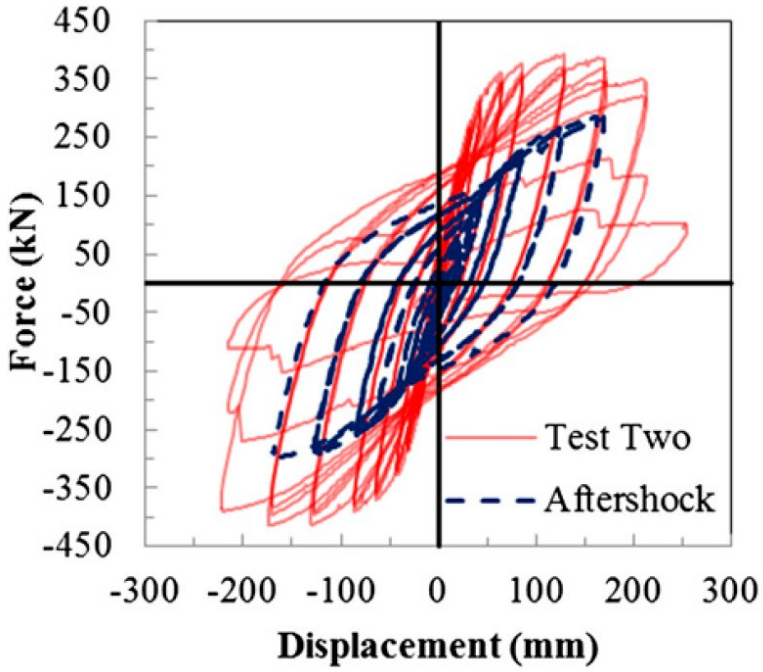

Figure 2.14 Experimental Test B: cyclic behavior of the original (Aftershock) and repaired (Test two) specimen (Rutledge et al. 2014)

2.4.2 Column numerical model and validation

Both the original and repaired columns were modeled as non-linear beam column elements with a fiber cross-section consisting of 12 subdivisions (fibers) in the circumferential direction and 24 subdivisions (fibers) in the radial direction. Figure 2.14 shows the column model and cross-section discretization. The repaired column, represented in figure 2.15, was reinforced using vertical and horizontal sheets of CFRP. Therefore, the cross-section was subdivided in regions: the cover confined by the CFRP jacket, and the core confined by both transverse reinforcement and the CFRP jacket. Tested values of the material properties, reported in table 2.1, were used to model the stress-strain curve for the reinforcing bars and effect of CFRP confinement. Since the repair strategy used by Rutledge et al. (2014) aimed to repair RC bridge columns by plastic hinge relocation, and given the promising result of their test confirmed

by figure 2.13, the lower portion of the RC repaired column was modeled with increased stiffness and strength.

Table 2.1 Test B: Material Properties

Longitudinal steel		Transverse steel	Concrete	Composite CFRP sheets		CFRP anchors	
Yield (MPa)	Ultimate (MPa)	Yield (MPa)	f'_c (MPa)	Tensile Strength (MPa)	Tensile Modulus (GPa)	Tensile Strength (MPa)	Tensile Modulus (GPa)
469	654	511	42.1	834	82	745	61.5

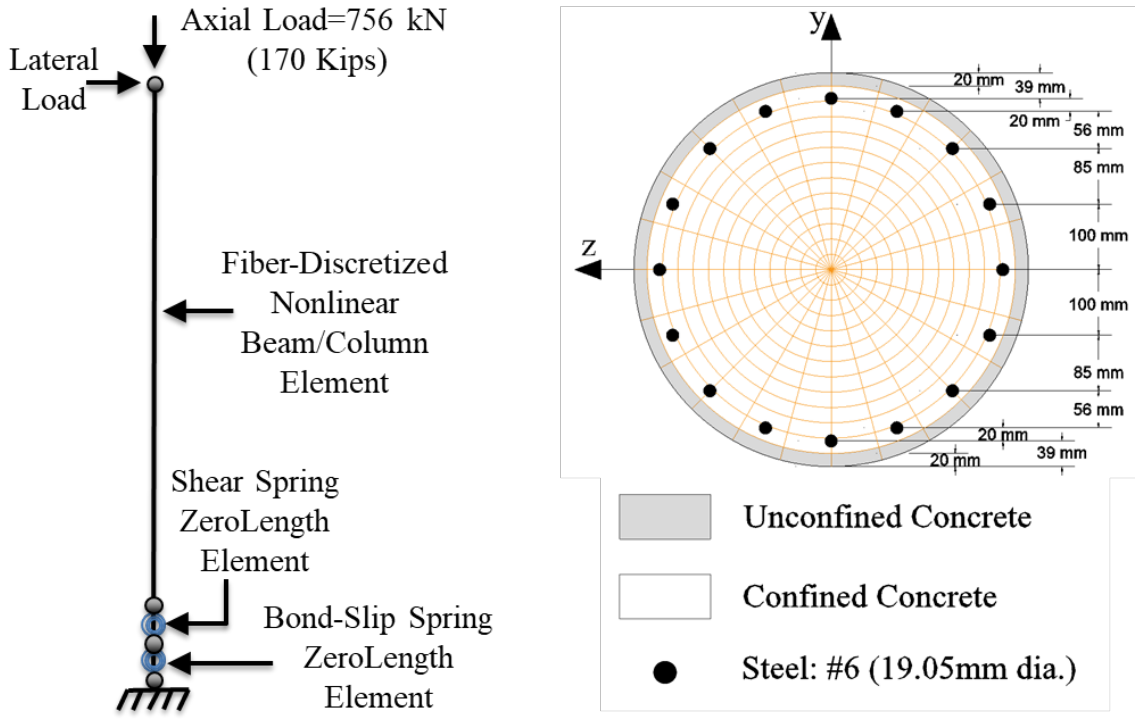

Figure 2.15 Test B: original column and cross section model

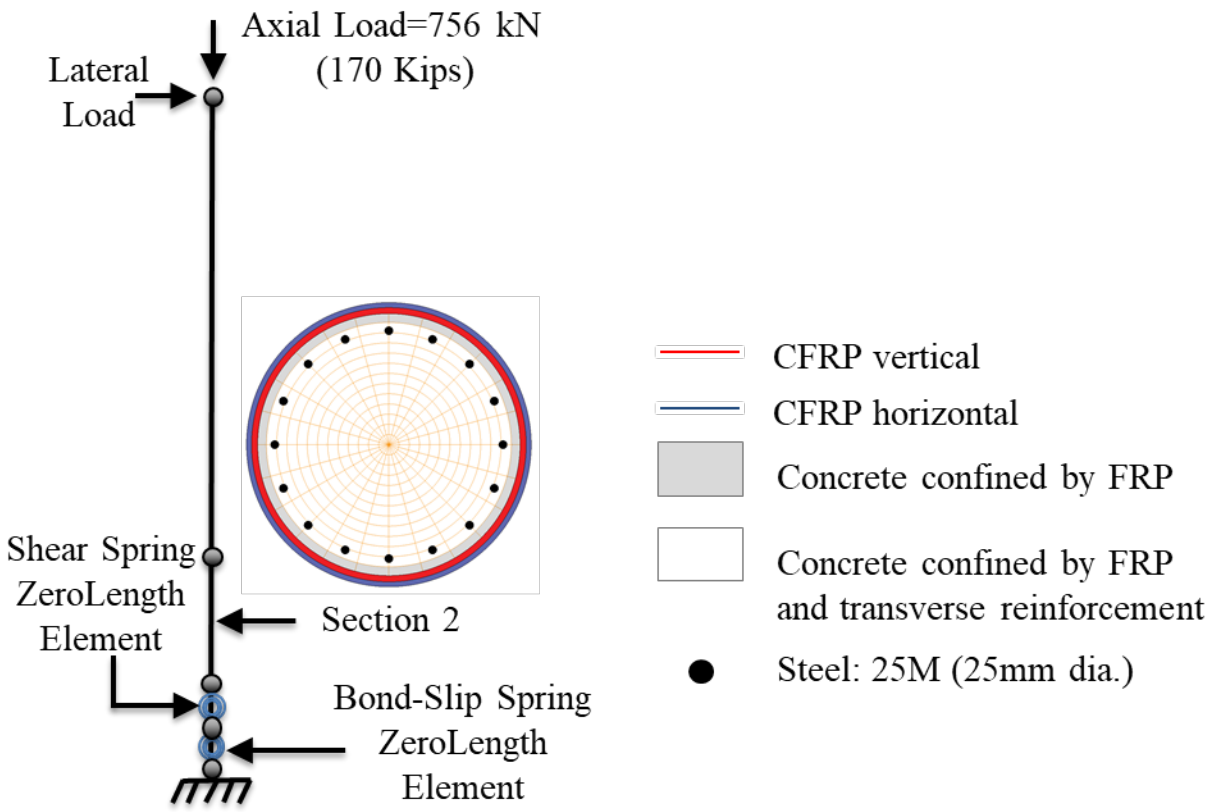

Figure 2.16 Test B: repaired column and cross section model

The experimental cyclic test carried out on Test B was modeled in OpenSees according to the description in Section 2.2. The software was run on a workstation with an Intel Xenon processor with a speed of 3.6 GHz on a 64-b operating system. The program took approximately 1 minute. The analysis graphs presented below were obtained by plotting OpenSees output text files using MATLAB. In figure 2.16 and 2.17 the numerical results of Test B are shown and compared with the experimental backbone curves. These results show the repaired column can be simulated using the proposed approach.

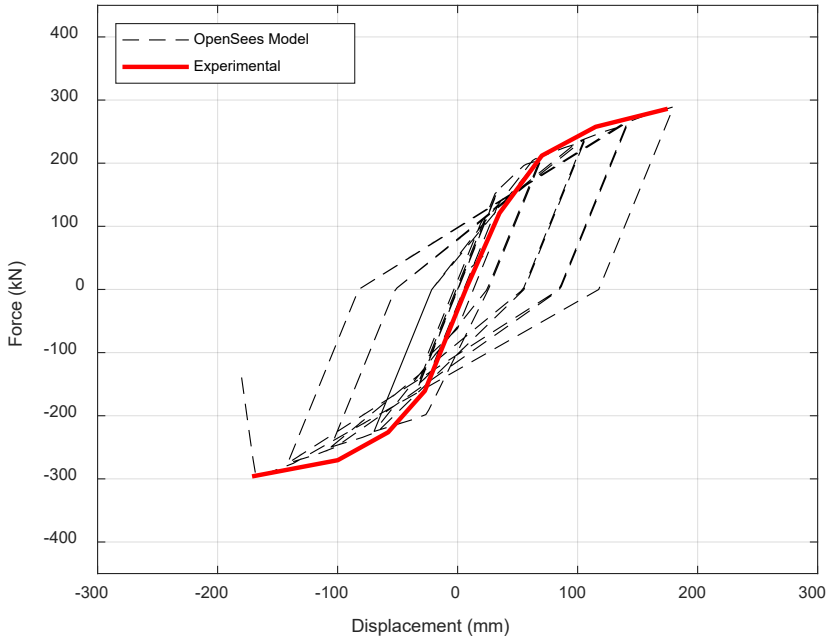

Figure 2.17 Test B: numerical and experimental cyclic behavior of original column

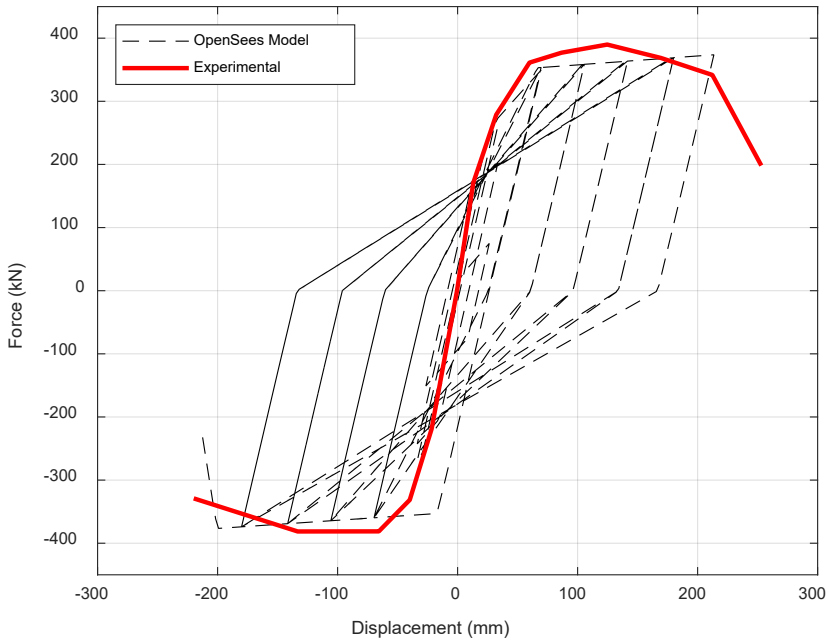

Figure 2.18 Test B: numerical and experimental cyclic behavior of repaired column

Chapter 3 Behavior of RC Bridge Structure

3.1 Overview

This section presents the numerical results of the RC bridge structure models with undamaged (original) and repaired columns considered in this study. A prototype bridge was selected to be modeled using the Open System for Earthquake Engineering Simulation (OpenSees) software framework (McKenna et al. 2000). The original and corresponding repaired bridge column models developed in Chapter 2 were implemented into the bridge structure model in different locations with the intent to evaluate the post-repair seismic response of the bridge structure with different numbers and locations of repaired columns. Ground motion records were selected from the Pacific Earthquake Engineering Research Center (PEER) Strong Motion Database and applied to the bridge structure model using incremental dynamic analysis (IDA). The aim of the dynamic analysis was to generate IDA curves of the intensity measure (IM) vs. damage measure (DM) for the selected ground motion records. A 5% damped first mode spectral acceleration Sa(T1,5%) (where T1 is the period of the 1^{st} mode response) was adopted as the IM, and the maximum drift ratio was adopted as the DM. The methodology adopted in this study was previously established by He et al. (2016) and was extended in this work to investigate the performance of different RC column repair systems.

3.2 RC Bridge Structure Model and Validation

A three-span RC bridge structure provided by the Federal Highway Administration named *Seismic Design of Bridges – Design Example No. 4* (FHWA 1996) was modeled in OpenSees. The bridge had RC columns with a geometry (in terms of cross-sectional shape and aspect ratio) similar to those simulated in Chapter 2. The superstructure was designed with continuous bents of 100 ft. (30.5 m), 120 ft. (36.6 m), and 100 ft. (30.5 m). The 30-degree skew

between the superstructure and bents was not considered since the skew effect was not the focus of this study. Figure 3.1 shows an illustration of the prototype bridge model.

The RC bridge columns had a height of 20 ft. (6.1 m) and a circular cross-section with 48 in. (1.22 m) diameter. The columns were reinforced with 34 ASTM 706 Grade 60 No. 11 (35 mm dia.) longitudinal bars, and No. 5 (16 mm dia.) spirals at a spacing of 3.5 in. (89 mm) with a concrete cover of 2 in. (50 mm). The resulting longitudinal and transverse reinforcing ratios were 2.79% and 0.8%, respectively. The effective height of the columns was 23.38 ft. (7.13 m) from the top of the footing to the centroid of the gross cross-section of the box girder, with a resulting aspect ratio of 5.85 for the columns. According to the design example (FHWA 1996), the bridge was designed for seismic loading using the Standard Specification for Highway Bridges (AASHTO 1995). The bent columns were designed to be cast in place (CIP) monolithically with the CIP box girder resulting in nearly fixed joint between the superstructure and the substructure.

The bridge was modeled using OpenSees with a 1/2–scale to be adapted to fit the dimensions of the RC columns chosen previously (Chapter 2). The superstructure model consisted of 12 elements, four elements per span, located in a single line along the centerline of the bridge structure. The moment of inertia and the torsional stiffness of the superstructure were determined based on gross cross-sectional properties. The mass density of the superstructure was adjusted so the fundamental frequency remained the same as the full-scaled bridge. Figure 3.2 shows the numerical model of the scaled bridge structure in OpenSees. This model was used in the simulation of an RC bridge with repaired columns to study how the repair influences the system response, where the original and repaired column models discussed in Chapter 2 were to be used for the bridge column elements (as discussed in Section 3.3).

For simplification purposes, the analysis focused on the response of the bridge structure in a single direction corresponding to the predominant direction of the response.

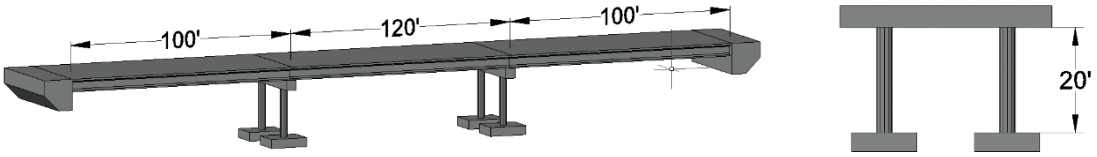

Figure 3.1 Design example No. 4 bridge dimensions (1 ft. = 0.3048 m)

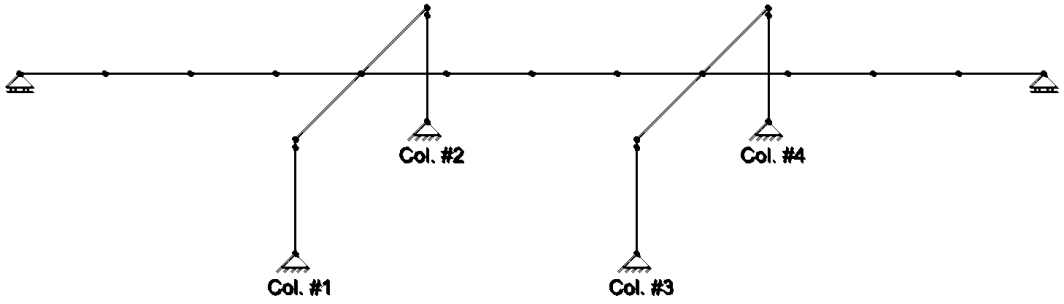

Figure 3.2 Numerical model of the scaled bridge structure

Modal analysis was conducted to validate the numerical bridge model. The fundamental frequency of the model including only original columns determined from the modal analysis was 1.236 Hz, which is similar to the value provided for the full-scaled bridge in the example No. 4 (1.202 Hz).

PROGRAM SAP90, VERSION BETA6.00 FILE:exam4.OUT
FHWA BRIDGE NO 4 PRELIMINARY DESIGN CALCS

E I G E N V A L U E S A N D F R E Q U E N C I E S

MODE	PERIOD (TIME)	FREQUENCY (CYC/TIME)	FREQUENCY (RAD/TIME)	EIGENVALUE (RAD/TIME)**2
1	0.831827	1.202172	7.553472	57.054941
2	0.492683	2.029703	12.753000	162.639019
3	0.297626	3.359927	21.111042	445.676084
4	0.229760	4.352366	27.346720	747.843098
5	0.208742	4.790611	30.100294	906.027677
6	0.204992	4.878243	30.650903	939.477861
7	0.125186	7.988121	50.190842	2519.121
8	0.101884	9.815115	61.670188	3803.212
9	0.082165	12.170569	76.469940	5847.652
10	0.081362	12.290709	77.224804	5963.670
11	0.076875	13.008090	81.732243	6680.160
12	0.068666	14.563152	91.502984	8372.796

Figure 3.3 Example No. 4 modal periods and vibrations (FHWA 1996)

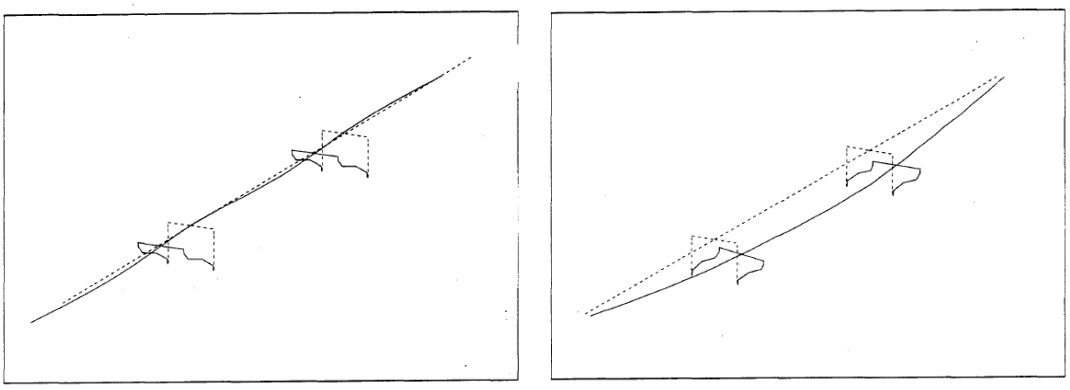

Figure 13 – Deformed Shape for Mode 1

Figure 14 – Deformed Shape for Mode 2

Figure 3.4 Example No. 4 deformed shapes for mode 1 (left) and mode 2 (right) (FHWA 1996)

3.3 Modeling of RC Bridge Structure with Repaired Columns

3.3.1 Models considered

Similar to the study by He et al. (2016), the analysis was conducted for the prototype bridge structure using seven different models to consider different scenarios of repaired columns. For each repair system studied, the pairs of original and corresponding repaired bridge column

models developed in Chapter 2 were implemented into the seven bridge structure models as follows. The original bridge structure model using all original columns (i.e., without repaired columns) was used as the control and is referred to as model Orig. The bridge structure models with different scenarios of repaired columns are referred as models R-1, R-12, R-13, R-14, R-123, and R-1234, where R indicates the model included one or more repaired column elements, and the numbers 1,2,3,4 identify the columns that were repaired in the model. Column numbers are defined in figure 3.2. The other columns in each model were modeled as original columns.

Results of models R-1, R-12 (or R-13 or R-14), R-123, and R1234, which had 1, 2, 3, and 4 repaired columns, respectively, were used to study the influence of the number of repaired columns. Results of Models R-12, R-13, and R-14, each with two repaired columns, were used to study the influence of repaired column location.

3.3.2 Selection of ground motion records

Twenty data sets of GM records from seven earthquakes were selected according to the target design spectrum determined with (AASHTO 1995). Each data set included subsets of data in two orthogonal directions recorded from the same event and record station resulting in 40 total GM records. The GM records were obtained from the database provided by the Pacific Earthquake Engineering Research Center (PEER). The records were selected among those with relatively large magnitudes of 6.5–7.0 and with moderate epicentral distances of 15–31 km.

According to Bradley et al. (2006), the selected GM records were scaled to a spectral acceleration of 1.0 g at the fundamental time period of the structure. Table 2 shows the eartquake set with the relative PGA values. Figure 3.5 shows the spectral acceleration for the selected GM records before and after scaling.

Table 3.1 Selected earthquake ground motion records

Earthquake set	Event	Year	Station	Ma	Rrup (km)	Record no.	PGA (g)
1	San Fernando	1971	LA – Hollywood Stor FF	6.61	22.8	1	0.2248
						2	0.1949
2	Imperial Valley-06	1979	Cerro Prieto	6.53	15.2	3	0.1683
						4	0.1571
3	Imperial Valley-06	1979	Delta	6.53	22.0	5	0.2357
						6	0.3497
4	Imperial Valley-06	1979	El Centro Array #12	6.53	19.9	7	0.1449
						8	0.1181
5	Imperial Valley-06	1979	El Centro Array #13	6.53	22.0	9	0.1180
						10	0.1385
6	Irpinia -Italy -01	1980	Bisaccia	6.90	21.3	11	0.0955
						12	0.0825
7	Superstition Hills-02	1987	El Centro Imp. Co. Cent	6.54	18.2	13	0.3573
						14	0.2595
8	Superstition Hills-02	1987	Kornbloom Road (temp)	6.54	18.5	15	0.1139
						16	0.1390
9	Superstition Hills-02	1987	Wildlife Liquef. Array	6.54	23.9	17	0.1792
						18	0.2076
10	Spitak-Armenia	1988	Gukasian	6.77	24.0	19	0.2003
						20	0.1740
11	Loma Prieta	1989	Agnews State Hospital	6.93	24.6	21	0.1652
						22	0.1379
12	Loma Prieta	1989	Coyote Lake Dam (Downst)	6.93	20.8	23	0.1604
						24	0.1794
13	Loma Prieta	1989	Coyote Lake Dam (SW Abut)	6.93	20.3	25	0.1519
						26	0.4847
14	Loma Prieta	1989	Hollister – South & Pine	6.93	27.9	27	0.3699
						28	0.1787
15	Loma Prieta	1989	Hollister Diff. Array	6.93	24.8	29	0.2689
						30	0.2786
16	Loma Prieta	1989	Palo Alto – 1900 Embarc.	6.93	30.8	31	0.2146
						32	0.2047
17	Loma Prieta	1989	Palo Alto – SLAC Lab	6.93	30.9	33	0.1948
						34	0.2771
18	Loma Prieta	1989	Sunnyvale – Colton Ave.	6.93	24.2	35	0.2074
						36	0.2072
19	Northridge-01	1994	LA – Wadsworth VA Hospital North	6.69	23.6	37	0.1854
						38	0.1642
20	Northridge-01	1994	Playa Del Rey – Saran	6.69	24.4	39	0.1435
						40	0.0701

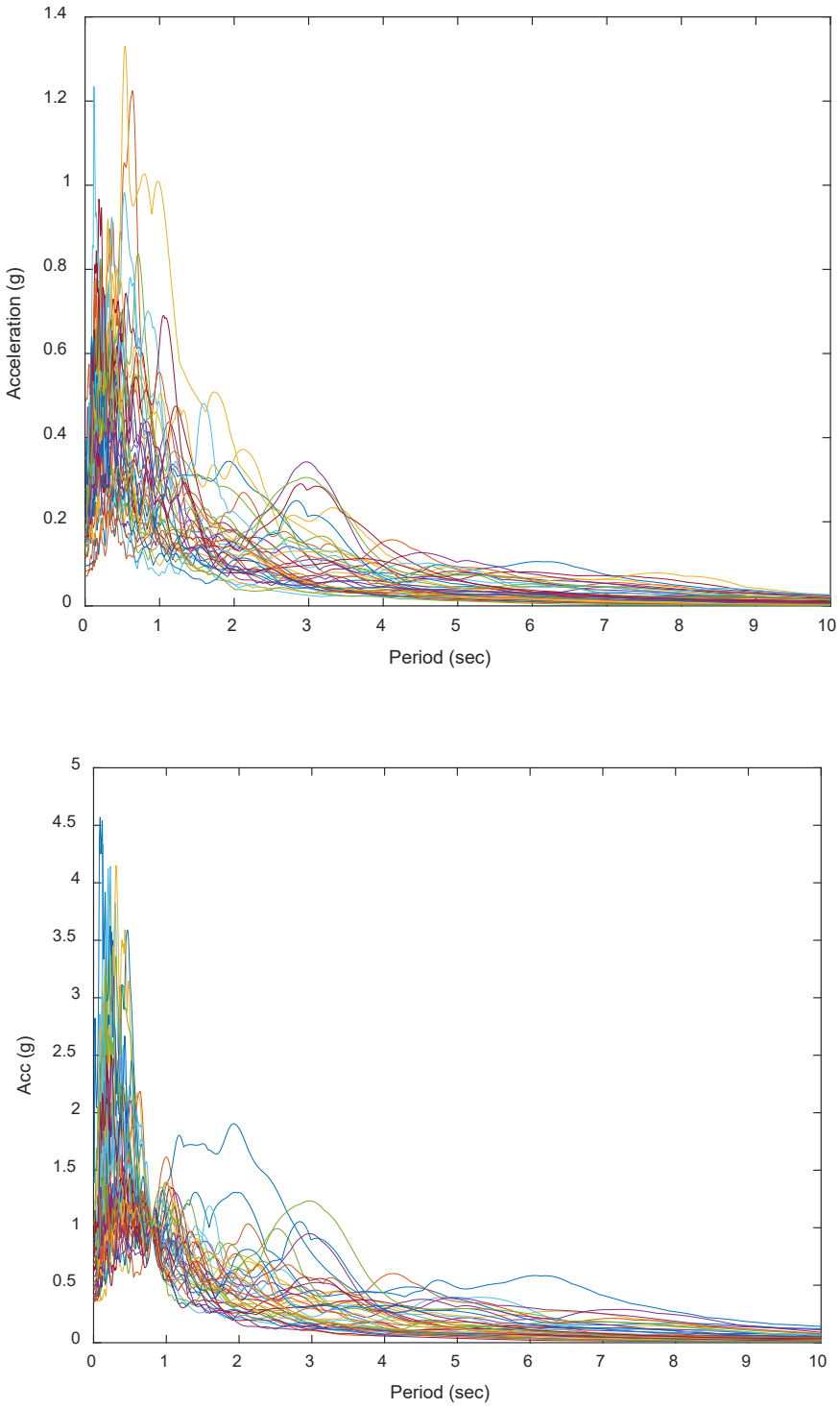

Figure 3.5 Spectral acceleration for the selected GM records before (top) and after scaling (bottom).

3.3.3 Incremental dynamic analysis (IDA)

Incremental dynamic analysis (IDA) was conducted to evaluate the post-repair seismic performance of the prototype bridge structure with one or more repaired columns. Although currently IDA is not widely used in practice due to high computational demand, the availability of increasingly powerful computers and algorithms makes it a promising and increasingly effective tool. IDA enables a thorough and systematic evaluation of the seismic performance of structures because it considers a wide range of ground motions with different frequency content and different levels of intensity.

The development of the IDA method and details regarding the concepts were described in detail by Vamvatsikos and Cornell (2002). Accordingly, the following procedure was used to generate the IDA curves of the bridge models: (1) scaling each of the 40 selected GM records with an increment 0.1 g from zero to a value where numerical non-convergence of the dynamic analysis on the models occurred; (2) recording the maximum drift ratio at the top of the columns under the scaled records, while in the case of non-convergence the maximum drift ratio was set as infinity; and (3) plotting the relationship between the intensity measure (Sa (T1, 5%)) and the damage measure (maximum drift ratio) (He et al. 2016). Each point on each IDA curve is the result of a single dynamic analysis for the bridge model subjected to a single scaled GM.

The analysis was entirely carried out using the OpenSees framework, while the output was processed using the software MATLAB. This approach was different than that used by He et al. (2016), who used OpenSees in combination with a program developed in MATLAB to conduct the IDA, and then processed the output using MATLAB. This new approach was made possible by recent updates to the OpenSees framework to conduct IDA. A desktop computer

with twelve logical processors was used to conduct the IDA of fourteen bridge models. It should be noted that the IDA method is analytically intensive, requiring many nonlinear analyses.

The IDA curves of the seven bridge models with original and/or repaired columns from Experimental Test A (Section 2.3) are shown in figure 3.6. The IDA curves of the seven bridge models with original and/or repaired columns from Experimental Test B (Section 2.4) are shown in figure 3.7. Each solid line in figures 3.6 and 3.7 represents the relationship between Sa (T1, 5%) and the drift ratio demand on the columns for each GM record. The horizontal portion of each IDA curve represents the instability or non-convergence of analysis of the bridge model, i.e., at the corresponding Sa (T1, 5%) the structure may have collapsed. The results are discussed in Section 3.3.4.

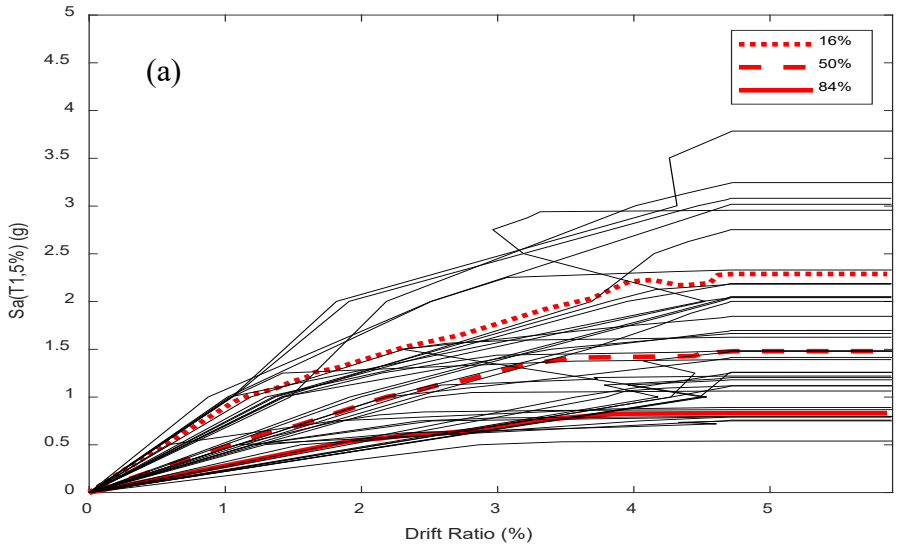
(a)
16%
50%
84%
Sa(T1,5%) (g)
Drift Ratio (%)

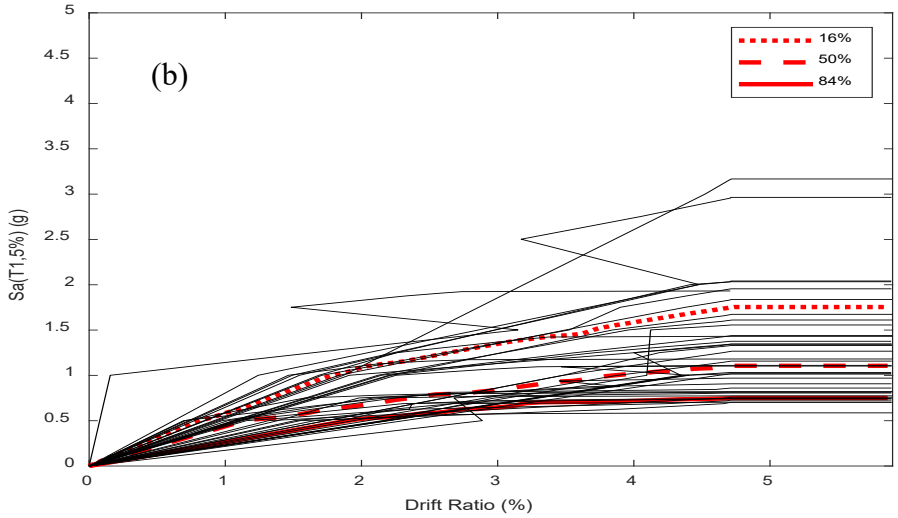
(b)
16%
50%
84%
Sa(T1,5%) (g)
Drift Ratio (%)

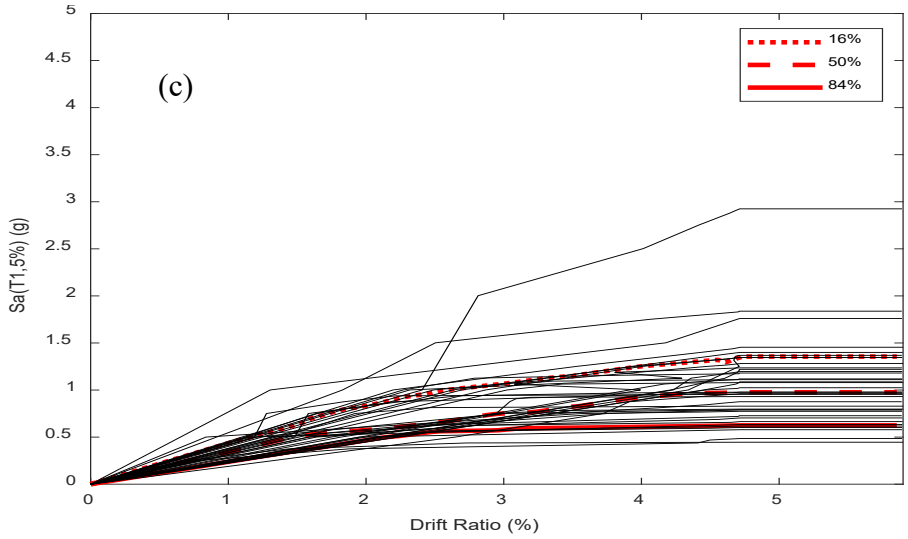
(c)
16%
50%
84%
Sa(T1,5%) (g)
Drift Ratio (%)

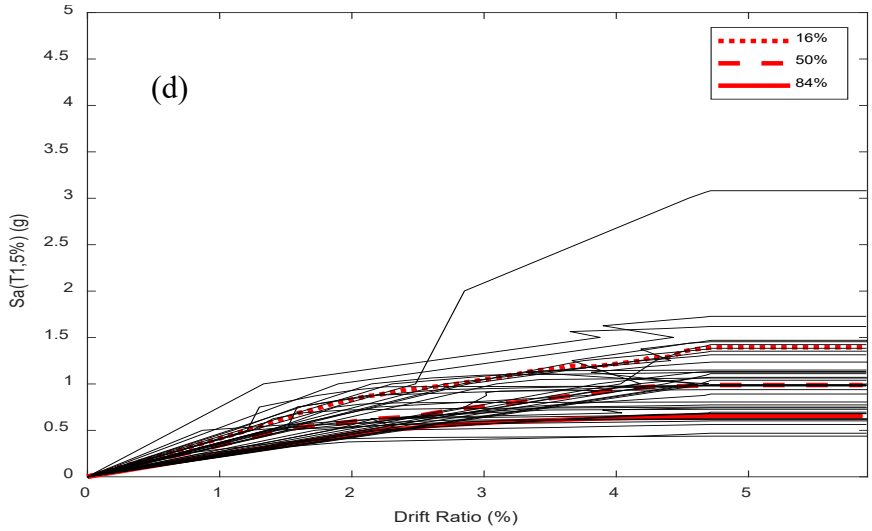
(d)
16%
50%
84%
Sa(T1,5%) (g)
Drift Ratio (%)

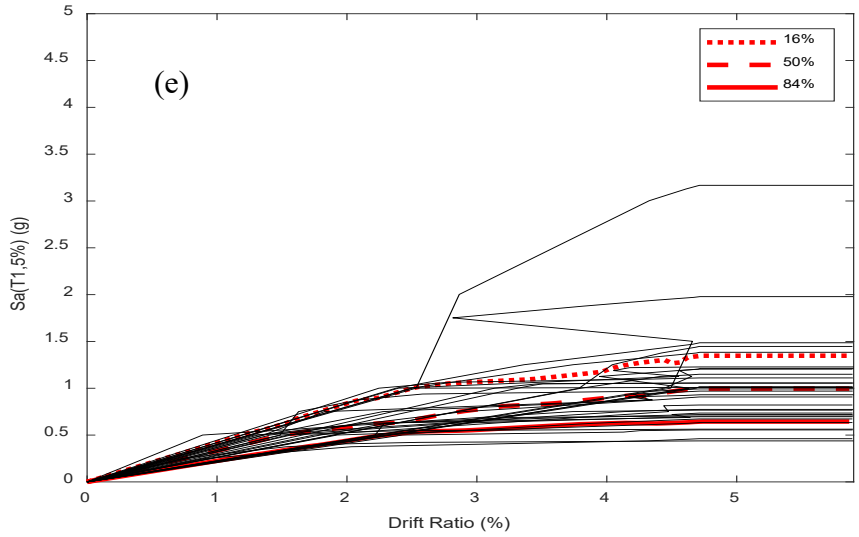
(e)
16%
50%
84%
Sa(T1,5%) (g)
Drift Ratio (%)

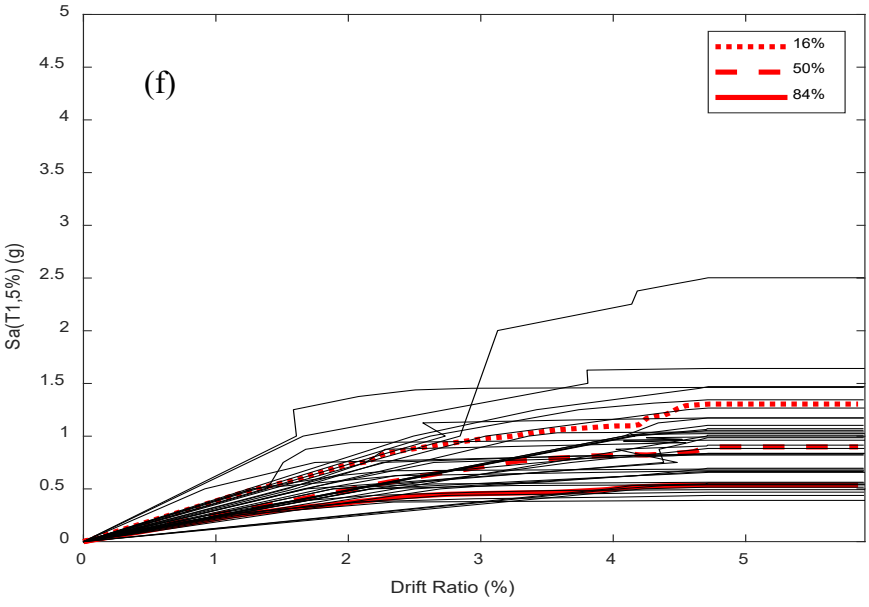
(f)
16%
50%
84%
Sa(T1,5%) (g)
Drift Ratio (%)

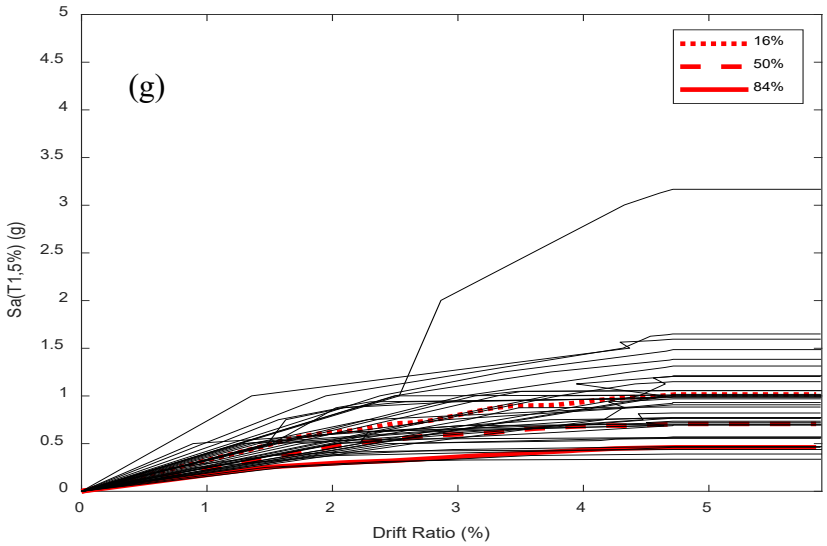

Figure 3.6 Experimental Test A: IDA curves of 40 GM records and 16th, 50th, and 84th percentiles: (a) Orig.; (b) R-1; (c) R-12; (d) R-13; (e) R-14; (f) R-123; (g) R-1234.

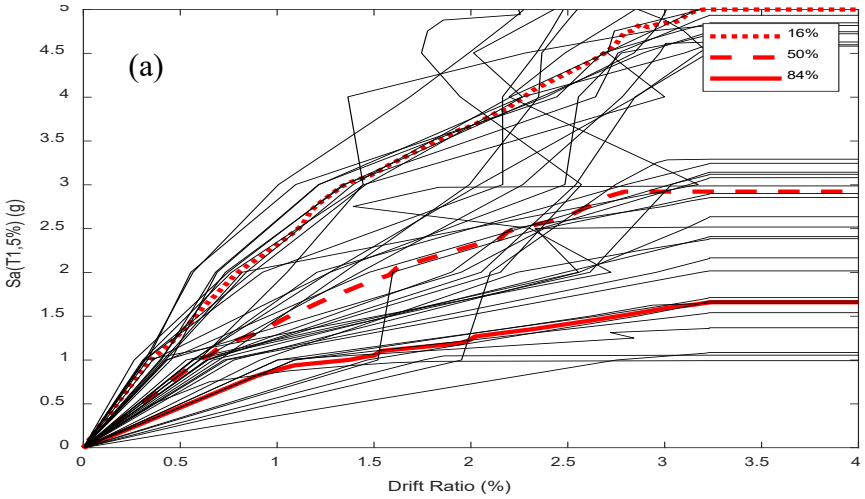
(a)
16%
50%
84%
Sa(T1,5%) (g)
Drift Ratio (%)

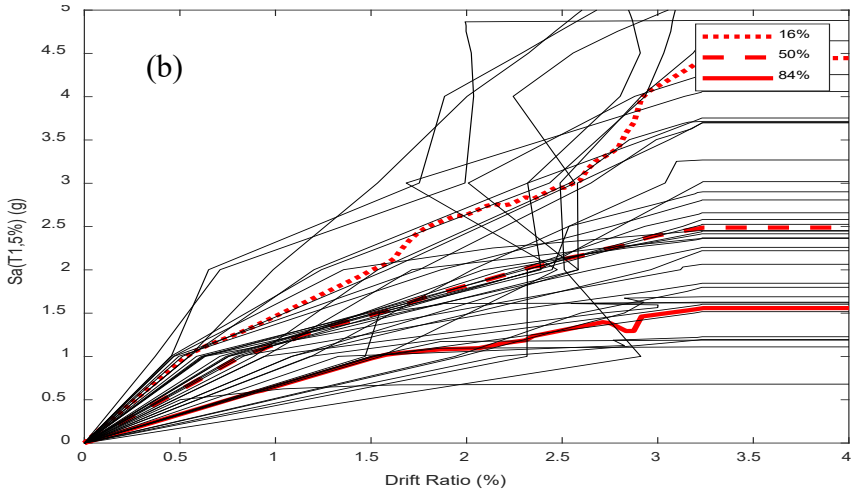
(b)
16%
50%
84%
Sa(T1,5%) (g)
Drift Ratio (%)

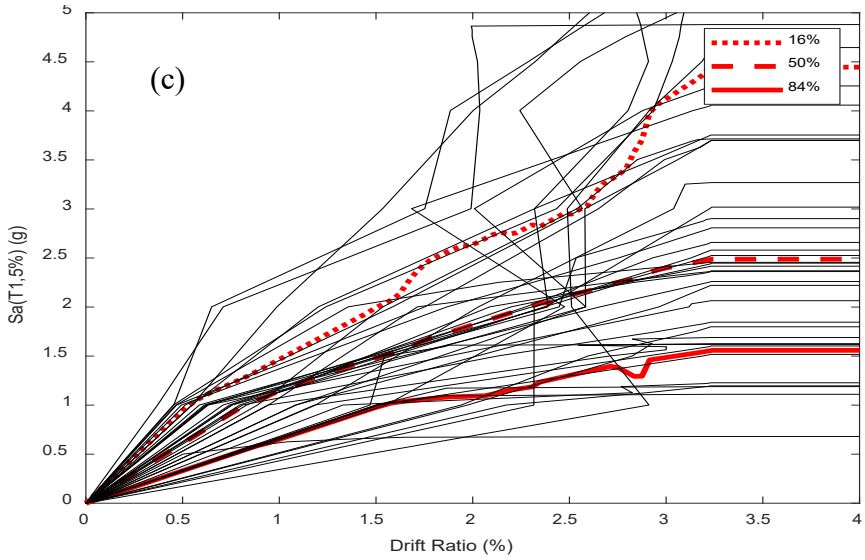
(c)
16%
50%
84%
Sa(T1,5%) (g)
Drift Ratio (%)

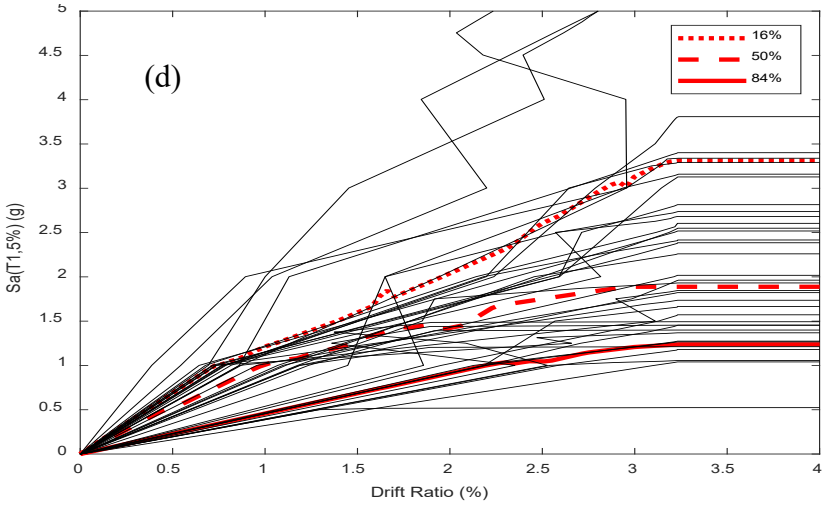
(d)
16%
50%
84%
Sa(T1,5%) (g)
Drift Ratio (%)

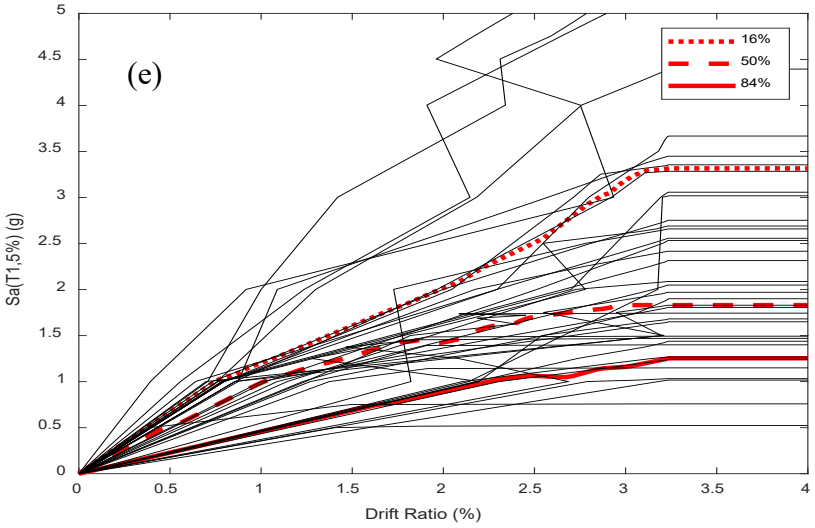
(e)
16%
50%
84%
Sa(T1,5%) (g)
Drift Ratio (%)

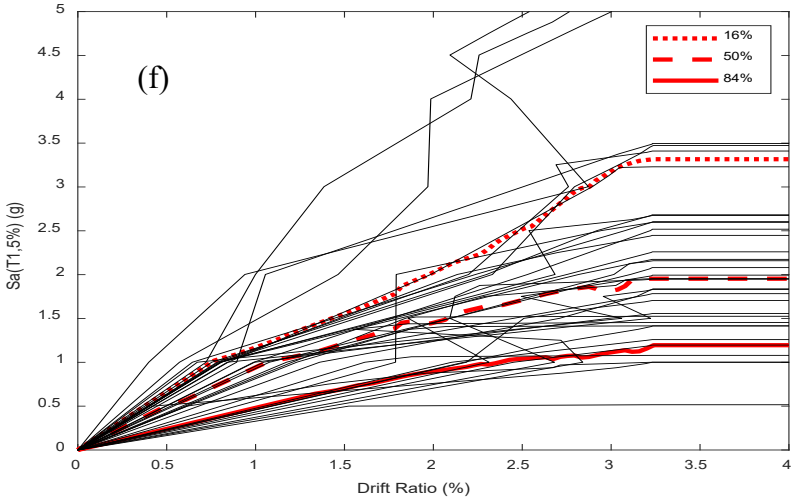
(f)
16%
50%
84%
Sa(T1,5%) (g)
Drift Ratio (%)

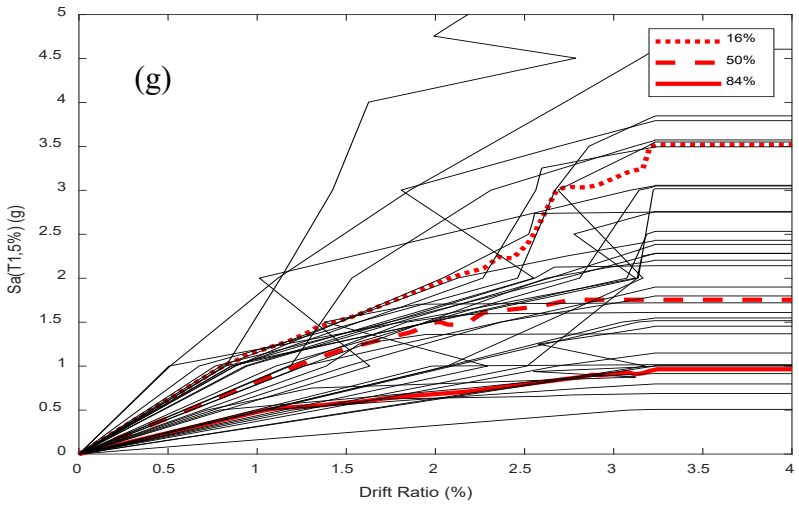

Figure 3.7 Experimental Test B: IDA curves of 40 GM records and 16th, 50th, and 84th percentiles: (a) Orig.; (b) R-1; (c) R-12; (d) R-13; (e) R-14; (f) R-123; (g) R-1234**.**

3.3.4 Summary and discussion

Figures 3.6 and 3.7 show the IDA curves of the seven bridge models with original and/or repaired columns from Experimental Tests A and B, respectively. In each figure, the set of IDA curves (corresponding to the 40 GM records) were summarized into curves corresponding to the 16th, 50th, and 84th percentiles, in which for a given Sa (T1, 5%) the percentile of all drift ratio demands to the left of the curve was 16%, 50%, and 84%, respectively. The percentile curves in figure 3.6a–g and 3.7a-g show that with an increasing number of repaired columns, the initial slope of the curve decreases, which corresponds to the decreasing initial stiffness of the bridge structure.

Results of the IDA show the seismic performance of the RC prototype bridge is only slightly affected by substituting the original columns with the repaired columns considered, therefore proving the effectiveness of two different repair strategies considered in this study. Figures 3.6 and 3.7 also show for both repair systems considered, i.e., Experimental Tests A and

B, the percentile curves for R-12, R-13, and R-14 are similar. This result suggests the location of the repaired columns does not significantly impact the behavior of the bridge models with the same number of repaired columns. These findings are similar to those by He et al. (2016) who simulated the same prototype bridge but with different original and repaired columns (in terms of column cross-section, damage condition, and repair method) than those in the present study.

Chapter 4 Conclusions

In this study, numerical simulation was used to model the response of two original (undamaged) and repaired reinforced concrete (RC) columns reported in the literature. The column models were implemented into the numerical model of a prototype bridge that was subjected to earthquake loading. Incremental dynamic analysis (IDA) was conducted on numerical bridge models to evaluate the efficacy of the column repair and the post-repair seismic performance of the prototype bridge that included one or more repaired columns. The methodology adopted in this study was based on previous work by He et al. (2016), in which the goal was to determine whether the reduced performance of a repaired column was acceptable for the overall performance of the repaired bridge. In the present study, the method was extended to columns with different repair conditions.

The original and repaired numerical models presented in this report were developed in OpenSees and validated against experimental data. The three-span RC prototype bridge was also modeled in OpenSees and validated using a design example reported in the literature. The IDA was conducted on the prototype bridge model that incorporated the developed column models employing 40 ground motion (GM) records, which were selected and scaled according to the target design response spectrum. The analysis was entirely carried out using the OpenSees framework, while the output was processed using the software MATLAB. This approach was different than that used by He et al. (2016), who used OpenSees in combination with a program developed in MATLAB to conduct the IDA, and then processed the output using MATLAB.

Results of this work showed the response of unrepaired RC columns was reproduced numerically using a classic approach with negligible discrepancy in terms of initial stiffness, base shear capacity, strength degradation, and stiffness degradation. Although similar, modeling

the response of repaired RC columns required a thorough evaluation of the pre-repair and post-repair damage state, as well as the repair design in order to accurately simulate the response.

Results of the IDA showed the seismic performance of the RC prototype bridge was only slightly affected by substituting the original columns with the repaired columns considered, therefore proving the effectiveness of two different repair strategies considered in this study. Within their group, test results of bridges with the same number of repaired columns but in different locations were comparable, suggesting overall response is not affected by the location of the repaired columns. To confirm this observation, valid for bridges with both Experimental Test A and Test B columns and for the columns considered in He et al. (2016), further investigation carried out on different bridge configurations is needed.

References

AASHTO (1995). “Standard Specifications for Highway Bridges, 15th ed”. *American Association of Highway Transportation Officials, Washington, D.C.*

American Concrete Institute – Committee 440 (2017). Guide for the Design and Construction of Externally Bonded FRP Systems for Strengthening Concrete Structures, ACI 440.2R-17, ACI, Farmington Hills, MI.

Bentz, E. C., & Collins, M. P. (2000). Response 2000. *Reinforced Concrete Sectional Analysis using the Modified Compression Field Theory, Version*, *1*(5).

Bradley, B., Dhakal, R., & Mander, J. B. (2006). Dependency of Building Fragility to source mechanisms of records selected for Incremental Dynamic Analysis.

Fakharifar, M., Chen, G., Sneed, L., and Dalvand, A. (2015). “Seismic performance of post-mainshock FRP/steel repaired RC bridge columns subjected to aftershocks.” *Composites Part B: Engineering*, *72*, 183-198.

FHWA (1996). "Seismic design of bridges—Design example no. 4: Three-span continuous CIP concrete bridge." *Publication No. FHWA-SA-97-009*.

French, C. W., Thorp, G. A., and Tsai, W. J. (1990). “Epoxy repair techniques for moderate earthquake damage”. *ACI Structural Journal*, *87*(4), 416-424.

Fukuyama, K., Higashibata, Y., and Miyauchi, Y. (2000). “Studies on repair and strengthening methods of damaged reinforced concrete columns.” *Cement & Conc. Compos.,* 22: 81-88.

Goodnight, J. C., Feng, Y., Kowalsky, M. J., and Nau, J. M. (2012). “The effect of load history on reinforced concrete bridge column behavior.” *Final Rep. to AUTC and AKDOT, No. FHWA-AK-RD-12-09, Alaska Univ. Transportation Center, Fairbanks, AK.*

He, R., Sneed L. H., and Belarbi A. (2013). “Rapid repair of severely damaged RC columns with different damage conditions: an experimental study,” *International Journal of Concrete Structures. and Materials*, 7: 35–50.

He, R., Yang, Y., and Sneed, L. H. (2016). “Post-repair seismic assessment of RC bridges damaged with fractured column bars–A numerical approach.” *Engineering Structures*, *112*, 100-113.

Kent DC, Park P (1971). “Inelastic behavior of reinforced concrete members with cyclic loading*”. Bull NZ Soc Earthq Eng*. 4(1):108–25.

Lehman, D.E., Gookin, S.E., Nacamuli, A.M., and Moehle, J. P. (2001). “Repair of earthquake-damaged bridge columns”. *ACI Structural Journal,* 98: 233-242.

Mander, J. B., Priestley, M. J., and Park, R. (1988). “Theoretical stress-strain model for confined concrete.” *Journal of Structural Engineering*, *114*(8), 1804-1826.

Mazzoni, S., McKenna, F., Scott, M. H., & Fenves, G. L. (2006).” OpenSees command language manual”. *Pacific Earthquake Engineering Research (PEER) Center*, *264*.

McKenna, F., Fenves, G. L., and Scott, M. H. (2000). “Open system for earthquake engineering simulation”. *University of California, Berkeley, CA.*

Paulay, T., & Priestley, M. N. (1992). “Seismic design of reinforced concrete and masonry buildings”. *New York: Wiley.*

PEER, Pacific Earthquake Engineering Research Center http://peer.berkeley.edu/peer_ground_motion_database [Accessed 05.20.21].

Rutledge, S. T., Kowalsky, M. J., Seracino, R., & Nau, J. M. (2014). “Repair of Reinforced Concrete Bridge Columns Containing Buckled and Fractured Reinforcement by Plastic Hinge Relocation.” *Journal of Bridge Engineering*, *19*(8).

Rutledge, S.T. (2012). “FRP Repair of Circular Reinforced Concrete Columns by Plastic Hinge Relocation”. *North Carolina State University.*

Scott BD, Park R, and Priestley MJN (1982). “Stress-strain behavior of concrete confined by overlapping hoops at low and high strain rates”. *ACI Journal Proceedings*; 79 (1):13–27.

Shao, Y., Aval, S., and Mirmiran, A. (2005). “Fiber-element model for cyclic analysis of concrete-filled fiber reinforced polymer tubes.” *Journal of Structural Engineering*, *131*(2), 292-303.

Sheikh, S. A., & Yau, G. (2002). “Seismic behavior of concrete columns confined with steel and fiber-reinforced polymers.” *Structural Journal*, *99*(1), 72-80.

Sneed, L. H., Fraioli, G., and Alabdulhady, M. (2019). “Guide for the Selection of Rapid Repair Systems for Earthquake-Damaged Reinforced Concrete Bridge Columns” *(No. 25-1121-0005-136-1). Missouri University of Science and Technology.*

Vosooghi, A. (2010). “Post-earthquake evaluation and emergency repair of damaged RC bridge columns using CFRP materials”. *University of Nevada, Reno.*

Vosooghi, A. and Saiidi, M. S. (2010). “Seismic damage states and response parameters for bridge columns.” *Special Publication*, *271*, 29-46.

Vosooghi, A., and Saiidi, M.S. (2009). “Rapid repair of high-shear earthquake-damaged RC bridge columns.” *Proc., 25th US-Japan Bridge Engineering Workshop*, Tsukuba, Japan.

Xiao, Y., and Ma, R. (1997). “Seismic retrofit of RC circular columns using prefabricated composite jacketing.” *Journal of Structural Engineering*, *123*(10), 1357-1364.

Vamvatsikos, D., & Cornell, C. A. (2002). “Incremental dynamic analysis”. *Earthquake Engineering & Structural Dynamics*, 31(3), 491-514.

Yau, G. (1998). “Repair and Strengthening of Columns with Fibre Reinforced Composites”. *University of Toronto*

Zhao, J., & Sritharan, S. (2007). “Modeling of strain penetration effects in fiber-based analysis of reinforced concrete structures”. *ACI Materials Journal*, *104*(2), 133.

Zhu, Z., Ahmad, I., and Mirmiran, A. (2006). “Fiber element modeling for seismic performance of bridge columns made of concrete-filled FRP tubes.” *Engineering Structures*, *28*(14), 2023-2035.